Applied Mathematics & Information Sciences
An International Journal

http://dx.doi.org/10.18576/amis/200119

Analytical and Numerical Solutions to a 1D Advection-Diffusion Equation with Exponentially Decaying Inlet Boundary Condition

Joseph K. Ansong * *and Ferdinard Obeng-Forson*

Department of Mathematics, University of Ghana, Legon, Accra, Ghana

Received: 7 Nov. 2025, Revised: 21 Dec. 2025, Accepted: 27 Dec. 2026
Published online: 1 Jan. 2026

Abstract: This paper presents analytic and numerical solutions to a one-dimensional advection-diffusion equation (ADE) in a bounded domain in which the inlet boundary condition is exponentially decaying. The Laplace transform technique is utilized to obtain the analytic solution and an optimal explicit scheme is used to obtain the numerical solution. One of the analytic solutions, which employs a relatively recent technique, is not continuous at the end points, while the solution derived here is continuous at the ends of the domain. The discrepancy between the two analytic solutions is explained. This paper also explains the correspondence between two different forms of the dimensionless ADE often presented in the literature, making it straightforward for comparisons of analytical and numerical solutions.

Keywords: Analytical, numerical, advection-diffusion, exponential boundary condition

1 Introduction

In a relatively recent study, [7] presented a general framework for deriving analytical solutions of the one-dimensional advection–diffusion equation (ADE) with constant coefficients via a one-sided Laplace transform method. The technique is relatively straightforward to apply, provided certain conditions are satisfied by the initial data and the inverse Laplace transform. Building on the approach of [7], analytical solutions to the one-dimensional ADE in a bounded domain with an exponentially decaying inlet boundary condition were derived in [12, 11]. However, the resulting analytical solution fails to satisfy the boundary conditions at both endpoints of the domain. In [12], the exponentially decaying inlet boundary condition was motivated by observational data obtained from a polluted river at Fenaso in the Ashanti Region of Ghana.

This paper derives an analytical solution to the one-dimensional ADE with an exponentially decaying inlet boundary condition using the Laplace transform, ensuring continuity at both endpoints. The solution is used to explain the source of the discrepancy between the continuous and discontinuous solutions. The continuous solution is consistent with that of [5] for a fixed inlet boundary condition. Among other significant uses, analytic solutions are generally useful for comparison to numerical solutions; to have an idea of the accuracy of a numerical method. Even though analytic solutions with discontinuities at one or both end points have been derived and utilized (e.g., [3] (section 4.7, page 144), [8, 7]), it is useful under many circumstances to obtain analytic solutions that are continuous at both end points.

In a recent study, [1] addressed a similar problem with an exponentially decaying inlet boundary condition, but employed a non-zero derivative boundary condition at the exit. Their results compared favorably with previous solutions that used a zero-derivative outlet condition, as well as with an explicit finite-difference numerical method. Moreover, their work corrected an error in a previously published analytical solution [13], which had applied a zero-gradient condition at the outlet.

The ADE (or transport equation) is often solved after non-dimensionalizing the equation and the corresponding boundary and initial conditions. Two forms of non-dimensional equations are often encountered in the literature; the native form where the resulting equation has a similar form as the dimensional equation (e.g., [4],

* Corresponding author e-mail: jkansong@ug.edu.gh

[9], [10]), and the Peclet form which results in a single coefficient in terms of the Peclet number (e.g., [2], [5], [7]). For purposes of analytical and numerical comparisons, it is useful to establish the correspondence between these two forms of the ADE. The relationship between these two forms is also presented in this paper. In addition, an explicit finite difference scheme originally derived by [9], is utilized for comparison and to illustrate the importance of having continuity at the boundary for analytic solutions.

Section 2 presents two forms of the non-dimensional ADE and we establish the relationship between them. Section 3 provides analytic solutions of the ADE via the technique of [7] and by directly applying the Laplace and inverse Laplace transforms. The solutions are reconciled through a Fourier series approach. A numerical method for solving the ADE is presented in section 4, and the results are discussed in section 5.

2 Background Theory

In Cartesian coordinates, the one-dimensional ADE is given by

$$\frac{\partial \phi}{\partial t} + u\frac{\partial \phi}{\partial x} = a\frac{\partial^2 \phi}{\partial x^2} \tag{1}$$

where a is a constant diffusion coefficient and u is the fluid velocity in the x direction respectively. Equation (1) represents a transport equation that models how heat or dissolved substances move within a fluid. The movement occurs through two main mechanisms: advection (or convection), which is transport due to the motion of the fluid, and diffusion (or conduction), which accounts for spreading caused by molecular processes. In heat transfer applications, $\phi(x,t)$ denotes the temperature, while in material transport problems it represents the concentration at position x and time t.

2.1 Non-dimensionalizations

2.1.1 Method 1

The coordinates of the transport equation will be non-dimensionalised so that the boundaries in each direction will be located at 0 and 1, the time will be non-dimensionalized so that a typical time period in the solution ϕ will be unity, and the speed of the fluid flow will be non-dimensionalized accordingly.

Let L be a typical length, such that $0 \le x \le L$. Replace the x variable by the dimensionless space variable

$$x_s = x/L \tag{2}$$

such that the domain is now defined by $0 \le x_s \le 1$. Let T be a characteristic interval of time associated with the given problem, such as the period of an oscillation in the dependent variable ϕ. Replace t by $t_s = t/T$, so that in terms of t_s the period of oscillation is now unity. Substitute the new independent variables x_s and t_s into (1) to get

$$\frac{\partial \phi}{\partial t_s} + \frac{uT}{L}\frac{\partial \phi}{\partial x_s} = \frac{aT}{L^2}\frac{\partial^2 \phi}{\partial x_s^2}. \tag{3}$$

We are left with non-dimensionalizing ϕ. Suppose ϕ_0 is a typical value of the dependent variable ϕ, then let $\phi_s = \phi/\phi_0$ and substitute into (3) to get

$$\frac{\partial \phi_s}{\partial t_s} + u_s\frac{\partial \phi_s}{\partial x_s} = \alpha\frac{\partial^2 \phi_s}{\partial x_s^2}, \tag{4}$$

where

$$u_s = uT/L,\ t_s = t/T,\ \alpha = \frac{aT}{L^2}. \tag{5}$$

Equation (4) is what we refer to as the native-form of the dimensionless ADE because it has the same form as the original equation (1).

The relative importance of advection with respect to diffusion is given by the Peclet number, Pe. It is typically established using scaling analysis of the advective and diffusive terms. For instance, if U, Φ, L and D are typical scales for u, ϕ, x, and α respectively, then

$$u\frac{\partial \phi}{\partial x} \sim U\frac{\Phi}{L} \text{ and } \alpha\frac{\partial^2 \phi}{\partial x^2} \sim D\frac{\Phi}{L^2}.$$

Therefore

$$Pe = \frac{\text{advection}}{\text{diffusion}} = \frac{U\Phi/L}{D\Phi/L^2} = \frac{UL}{D}.$$

2.1.2 Method 2

An alternative method of non-dimensionalizing the 1D ADE resulting in a single coefficient in terms of the Peclet number is presented next. Consider equation (1), and define

$$\left.\begin{array}{ll} \phi_b = \phi/\phi_0, & t_b = at/L^2, \\ x_b = x/L, & Pe = 2\lambda = Lu/a, \end{array}\right\} \tag{6}$$

where $0 \le x_b \le 1$. Substituting (6) into (1) yields:

$$\frac{\partial \phi_b}{\partial t_b} + Pe\frac{\partial \phi_b}{\partial x_b} = \frac{\partial^2 \phi_b}{\partial x_b^2}. \tag{7}$$

For mathematical convenience (7) is sometimes written in the form:

$$\frac{\partial \phi_b}{\partial t_b} + 2\lambda\frac{\partial \phi_b}{\partial x_b} = \frac{\partial^2 \phi_b}{\partial x_b^2}, \tag{8}$$

where $\lambda = Pe/2$.

2.1.3 Correspondence between the two non-dimensional forms

Comparing the two forms of the dimensionless ADE, we have $T = (\alpha L^2)/a$ such that

$$u_s = \frac{uT}{L} = \frac{u\alpha L}{a} \quad \Longrightarrow Pe = \frac{u_s}{\alpha} = \frac{uL}{a} \text{ and } \lambda = \frac{u_s}{2\alpha}. \tag{9}$$

Hence, the ratio of the coefficients in (4) yields the Peclet number in (7) or (8). Equation (9) partially relates the native-form of the ADE to the Peclet-form in (7) or (8). Since time in the two forms is non-dimensionalized differently, it is additionally important to find the relationship between their time variables before a complete comparison can be undertaken. From (5), we have

$$t_s = \frac{t}{T}, \quad T = \frac{\alpha L^2}{a} \Longrightarrow t_s = \frac{at}{\alpha L^2}, \tag{10}$$

and from (6), we have

$$t_b = \frac{at}{L^2}. \tag{11}$$

Hence, equations (10) and (11) yield

$$t_b = \alpha t_s. \tag{12}$$

In summary, given a scheme that solves the native-form of the dimensionless ADE,

$$\frac{\partial \phi}{\partial t} + u\frac{\partial \phi}{\partial x} = \alpha \frac{\partial^2 \phi}{\partial x^2}, \tag{13}$$

an equivalent method for solving the dimensionless Peclet-form,

$$\frac{\partial \phi}{\partial t_b} + 2\lambda \frac{\partial \phi}{\partial x} = \frac{\partial^2 \phi}{\partial x^2}, \tag{14}$$

and vice versa, is to employ the relations:

$$\lambda = \frac{u}{2\alpha} \text{ and } t_b = \alpha t. \tag{15}$$

3 Analytic solutions to a 1D ADE

Consider the dimensionless Peclet-form of the ADE:

$$\frac{\partial \phi}{\partial t} = \frac{\partial^2 \phi}{\partial x^2} - 2\lambda \frac{\partial \phi}{\partial x}, \quad 0 \le x \le 1, \tag{16}$$

subject to:

$$\phi(0,t) = \phi_0 e^{-\gamma t}, \quad t > 0 \tag{17}$$

$$\phi(1,t) = \phi_1, \qquad t > 0, \tag{18}$$

and initial condition

$$\phi(x,0) = \omega_0, \qquad 0 \le x \le 1. \tag{19}$$

Applying the Laplace transform to equation (16) and using the boundary conditions yields (see [12, 11]):

$$\begin{aligned} \Phi(x,p) = &\left[\frac{\phi_0 \sinh[\beta(1-x)]}{\sinh\beta}\right]\frac{e^{\lambda x}}{p+\gamma} \\ &+ \left[\frac{\phi_1 e^{-\lambda}\sinh(\beta x)}{\sinh\beta}\right]\frac{e^{\lambda x}}{p} \\ &- \left[\frac{\omega_0 \sinh[\beta(1-x)] + \omega_0 e^{-\lambda}\sinh(\beta x)}{\sinh\beta}\right]\frac{e^{\lambda x}}{p} \\ &+ \frac{\omega_0}{p}, \end{aligned} \tag{20}$$

where

$$\beta = \sqrt{\lambda^2 + p}, \tag{21}$$

and p is the Laplace transform variable. We split equation (20) into partial solutions of the form:

$$\Phi_{BC_1}(x,p) = \phi_0 e^{\lambda x}\left[\frac{\sinh\beta(1-x)}{(p+\gamma)\sinh\beta}\right], \tag{22}$$

$$\Phi_{BC_2}(x,p) = \phi_1 e^{\lambda x - \lambda}\left[\frac{\sinh(\beta x)}{p\sinh\beta}\right], \tag{23}$$

$$\Phi_{IC_1}(x,p) = -\omega_0 e^{\lambda x}\left[\frac{\sinh\beta(1-x)}{p\sinh\beta}\right], \tag{24}$$

$$\Phi_{IC_2}(x,p) = -\omega_0 e^{\lambda x - \lambda}\left[\frac{\sinh(\beta x)}{p\sinh\beta}\right], \tag{25}$$

$$\Phi_{IC_3}(x,p) = \frac{\omega_0}{p}. \tag{26}$$

Only the inverse Laplace transform of (20) (equivalently the set of equations (22)-(26)) is required to obtain the general solution $\phi(x,t)$. The inversion can be carried out by using a complex integral approach and investigation of the positioning of the poles of the function. In this case the poles occur at:

$$p = 0, \quad p = -\gamma, \tag{27}$$

$$\sinh(\beta) = 0, \tag{28}$$

and the inversion becomes the sum of the residues associated with these poles. For instance, the residue associated with a pole at $z = z_0$ for the function $\Phi_{BC_1}(x,p)$ can be found as

$$\lim_{z\to z_0}\left[(z-z_0)\Phi_{BC_1}(x,z)e^{zt}\right] = \phi_0 e^{x\lambda - z_0 t}\mathscr{R}[f_{BC_1}] \tag{29}$$

where p is replaced by the complex variable z, and $\mathscr{R}[f_{BC_1}]$ is the specific residue of Φ_{BC_1} to be determined for $z = z_0$. A technique introduced by [7] (see also [12], [11]) avoids finding the specific residues associated with the pole at $\sinh\beta = 0$, instead, they cleverly apply the

initial condition to get the final solution

$$\phi(x,t) = \phi_0 e^{\lambda x}\left[\frac{\sinh\lambda(1-x)}{\sinh\lambda}\right]\left(e^{-\gamma t}-e^{-\lambda^2 t}\right) + \phi_1 e^{\lambda x}\left[\frac{\sinh(\lambda x)}{\sinh\lambda}\right]\left(1-e^{-\lambda^2 t}\right)e^{-\lambda} - \omega_0 e^{\lambda x}\left(\frac{\sinh\lambda(1-x)+e^{-\lambda}\sinh(\lambda x)}{\sinh\lambda}\right)\times \left(1-e^{-\lambda^2 t}\right)+\omega_0. \quad (30)$$

This solution is consistent with that of [7] for $\gamma = 0$. However, the solution in (30) is discontinuous at the end points. Kim states that the discontinuities may be technically resolved using Fourier series, nevertheless, the discrepancy was not resolved for $\gamma = 0$. Kim refers to the Fourier series solution derived by [8] for $\gamma = 0$, $\phi_0 = 1$ and $\phi_1 = 0$. The paper by [5] corrects some mistakes in the solution of [8] though his paper appears to be less known in the literature. We later explain the source of the discontinuities in (30) after we determine a solution that is continuous at both end points. This is achieved by directly finding the inversions of (22)-(26) via tables of Laplace transforms (e.g., [6]), using the residue theorem, and employing a property of Laplace transforms that

$$\mathscr{L}^{-1}\{\hat{\phi}(x,p+b)\} = \exp(-bt)\mathscr{L}^{-1}\{\hat{\phi}(x,p)\}. \quad (31)$$

For equation (22), we have

$$\Phi_{BC_1}(x,p) = \phi_0 e^{\lambda x}\left[\frac{\sinh\sqrt{\lambda^2+p}(1-x)}{(p+\gamma)\sinh\sqrt{\lambda^2+p}}\right],$$

and replacing p by $p-\lambda^2$ gives

$$\Phi_{BC_1}(x,p-\lambda^2) = \phi_0 e^{\lambda x}\left[\frac{\sinh\sqrt{p}(1-x)}{(p-(\lambda^2-\gamma))\sinh\sqrt{p}}\right],$$

such that

$$\mathscr{L}^{-1}\{\Phi_{BC_1}(x,p)\} = e^{-\lambda^2 t}\mathscr{L}^{-1}\left\{\Phi_{BC_1}(x,p-\lambda^2)\right\}.$$

$$\therefore \mathscr{L}^{-1}\{\Phi_{BC_1}(x,p)\} = \phi_0 e^{\lambda x-\lambda^2 t}\mathscr{L}^{-1}\left\{\frac{\sinh\sqrt{p}(1-x)}{(p-(\lambda^2-\gamma))\sinh\sqrt{p}}\right\} \quad (32)$$

By referring to the table of integrals in [6] yields (see Appendix A.2)

$$\mathscr{L}^{-1}\{\Phi_{BC_1}(x,p)\} = \phi_0 e^{\lambda x}\left\{\frac{\sinh\omega(1-x)}{\sinh\omega}e^{-\gamma t} - 2\pi\sum_{n=1}^{\infty}\frac{n\sin(n\pi x)}{\omega^2+n^2\pi^2}e^{-(\lambda^2+n^2\pi^2)t}\right\} \quad (33)$$

where

$$\omega = \sqrt{\lambda^2-\gamma}.$$

Similarly, we have

$$\mathscr{L}^{-1}\{\Phi_{BC_2}(x,p)\} = \phi_1 e^{-\lambda(1-x)}\left\{\frac{\sinh\lambda x}{\sinh\lambda}+ 2\pi\sum_{n=1}^{\infty}\frac{(-1)^n n\sin(n\pi x)}{\lambda^2+n^2\pi^2}e^{-(\lambda^2+n^2\pi^2)t}\right\}$$

and using the relation $-n\sin[\pi(1-x)] = (-1)^n\sin(n\pi x)$, we get

$$\mathscr{L}^{-1}\{\Phi_{BC_2}(x,p)\} = \phi_1 e^{-\lambda(1-x)}\left\{\frac{\sinh\lambda x}{\sinh\lambda}- 2\pi\sum_{n=1}^{\infty}\frac{n\sin[n\pi(1-x)]}{\lambda^2+n^2\pi^2}e^{-(\lambda^2+n^2\pi^2)t}\right\}. \quad (34)$$

Also,

$$\mathscr{L}^{-1}\{\Phi_{IC_1}(x,p)\} = -\omega_0 e^{\lambda x}\left\{\frac{\sinh\lambda(1-x)}{\sinh\lambda}- 2\pi\sum_{n=1}^{\infty}\frac{n\sin(n\pi x)}{\lambda^2+n^2\pi^2}e^{-(\lambda^2+n^2\pi^2)t}\right\}, \quad (35)$$

$$\mathscr{L}^{-1}\{\Phi_{IC_2}(x,p)\} = -\omega_0 e^{-\lambda(1-x)}\left\{\frac{\sinh\lambda x}{\sinh\lambda}- 2\pi\sum_{n=1}^{\infty}\frac{n\sin[n\pi(1-x)]}{\lambda^2+n^2\pi^2}e^{-(\lambda^2+n^2\pi^2)t}\right\}, \quad (36)$$

$$\mathscr{L}^{-1}\{\Phi_{IC_3}(x,p)\} = \mathscr{L}^{-1}\left\{\frac{\omega_0}{p}\right\} = \omega_0. \quad (37)$$

Summing all the inverse Laplace transforms gives the final solution in the form

$$\phi(x,t) = \mathscr{L}^{-1}\{\Phi_{BC_1}\}+\mathscr{L}^{-1}\{\Phi_{BC_2}\}+\mathscr{L}^{-1}\{\Phi_{IC_1}\}+ \mathscr{L}^{-1}\{\Phi_{IC_2}\}+\omega_0, \quad (38)$$

such that, upon rearranging, we get

$$\phi(x,t) = e^{\lambda x}\left[\phi_0\frac{\sinh\omega(1-x)}{\sinh\omega}e^{-\gamma t}-\omega_0\frac{\sinh\lambda(1-x)}{\sinh\lambda}\right] +e^{-\lambda(1-x)}\frac{\sinh(\lambda x)}{\sinh\lambda}(\phi_1-\omega_0) +2\pi e^{\lambda x}\left[\omega_0\sum_{n=1}^{\infty}\frac{n\sin(n\pi x)}{\lambda^2+n^2\pi^2} -\phi_0\sum_{n=1}^{\infty}\frac{n\sin(n\pi x)}{\omega^2+n^2\pi^2}\right]e^{-(\lambda^2+n^2\pi^2)t} -2\pi e^{-\lambda(1-x)}(\phi_1-\omega_0)\times \left[\sum_{n=1}^{\infty}\frac{n\sin[n\pi(1-x)]}{\lambda^2+n^2\pi^2}e^{-(\lambda^2+n^2\pi^2)t}\right]+\omega_0. \quad (39)$$

The solution in equation (39) is continuous at both end points unlike equation (30). This is because, substituting $x = 0$ in (39) yields $\phi(0,t) = \phi_0 e^{-\gamma t}$ and substituting $x = 1$ gives rise to $\phi(1,t) = \phi_1$ as expected. It is possible to reconcile the two solutions given by (30) and (39) by using Fourier series expansions of the terms

$$\frac{\sinh[\lambda(1-x)]}{\sinh\lambda} \quad \text{and} \quad \frac{\sinh(\lambda x)}{\sinh\lambda}$$

that multiply the exponential terms $\exp(-\lambda^2 t)$ in (30), to give a solution that is continuous throughout the domain. However, it should be noted that the term $\exp(-\lambda^2 t)$, arising from the pole $\sinh\beta = 0$ (see equation (28)), should be $\exp[-(\lambda^2 + n^2\pi^2)t]$. This is because

$$\sinh\beta = \sinh\sqrt{\lambda^2+z} = -i\sin[i\sqrt{\lambda^2+z}] = 0,$$

$$\Longrightarrow \sqrt{\lambda^2+z} = -in\pi \Longrightarrow z = -(\lambda^2+n^2\pi^2),$$

instead of $z = -\lambda^2$ as employed in Kim's method. Also notice that the expressions in curly brackets in (33)-(36) vanish for $t = 0$ upon application of the Fourier series expansions of the ratio of sine hyperbolic functions, giving $\phi(x,0) = \omega_0$. So the resulting solution also satisfies the initial condition. The Fourier series expansions of the ratio of hyperbolic functions for $x \neq 0$ are (see Appendix A.1):

$$\frac{\sinh[\lambda(1-x)]}{\sinh(\lambda)} = 2\pi\sum_{n=1}^{\infty}\frac{n\sin(n\pi x)}{\lambda^2+(n\pi)^2}, \tag{40}$$

$$\frac{\sinh(\lambda x)}{\sinh(\lambda)} = 2\pi\sum_{n=1}^{\infty}\frac{n\sin[n\pi(1-x)]}{\lambda^2+(n\pi)^2}. \tag{41}$$

For $\gamma = 0$, $\phi_0 = 1$, $\phi_1 = 0$, and $\omega_0 = 0$, the solution converges to that of [5] (see also [7]; equation (24) in their supplementary information):

$$\phi(x,t) = e^{\lambda x}\left[\frac{\sinh\lambda(1-x)}{\sinh\lambda} - 2\pi\sum_{n=1}^{\infty}\frac{n\sin(n\pi x)}{\lambda^2+n^2\pi^2}e^{-(\lambda^2+n^2\pi^2)t}\right] \tag{42}$$

where we used the fact that $\omega = \sqrt{\lambda^2+\gamma} = \lambda$ for $\gamma = 0$.

We next carry out a numerical discretization of the ADE in its native form and establish the consistency and stability properties of the explicit numerical scheme to be employed. The numerical solution is later compared to the analytic solutions, to explain some shortcomings of analytic solutions which have discontinuities at the endpoints of the domain of interest.

4 Numerical discretization

Consider the native-form of non-dimensional ADE:

$$\frac{\partial\phi}{\partial t} + u\frac{\partial\phi}{\partial x} = \alpha\frac{\partial^2\phi}{\partial x^2} \tag{43}$$

for $0 < x < 1$ and $\phi(x,t)$, subject to initial condition

$$\phi(x,0) = w_0 \tag{44}$$

together with Dirichlet boundary conditions

$$\phi(0,t) = \phi_0 e^{-\gamma t}, \quad \phi(1,t) = \phi_1. \tag{45}$$

At the (j,n) grid point, the equation is discretized using a weighted-average method:

$$\frac{\partial\phi}{\partial t}\Big|_j^n + u\frac{\partial\phi}{\partial x}\Big|_j^n = \alpha\frac{\partial^2\phi}{\partial x^2}\Big|_j^n.$$

Here, the forward difference is used for the time derivative, the centered difference is applied to the second-order spatial derivative, and a weighted combination of backward and centered differences is employed for the first-order spatial derivative, namely

$$\frac{\partial\phi}{\partial x}\Big|_j^n = \psi\frac{\partial\phi}{\partial x}\Big|_j^n + (1-\psi)\frac{\partial\phi}{\partial x}\Big|_j^n, \quad 0 \le x \le 1. \tag{46}$$

The backward difference is used for the spatial derivative term with coefficient ψ, while the centered difference is applied to the term associated with the weight $(1-\psi)$, yielding (e.g., [9, 1]):

$$\frac{\phi_j^{n+1}-\phi_j^n}{\Delta t} + O\{\Delta t\} + u\left[\psi\left(\frac{\phi_j^n-\phi_{j-1}^n}{\Delta x} + O\{\Delta x\}\right) + (1-\psi)\left(\frac{\phi_{j+1}^n-\phi_{j-1}^n}{2\Delta x} + O\{(\Delta x)^2\}\right)\right] = \alpha\left[\frac{\phi_{j+1}^n - 2\phi_j^n + \phi_{j-1}^n}{(\Delta x)^2} + O\{(\Delta x)^2\}\right]. \tag{47}$$

Neglecting the terms of order $O\{\Delta t, \psi\Delta x, (1-\psi)(\Delta x)^2\}$ and rearrangeing yields the explicit finite difference equation:

$$\bar\phi_j^{n+1} = \left[s + \frac{1}{2}(1+\psi)c\right]\bar\phi_{j-1}^n + (1-2s-\psi c)\bar\phi_j^n + \left[s - \frac{1}{2}(1-\psi)c\right]\bar\phi_{j+1}^n \tag{48}$$

where $j = 1, 2, \cdots, J-1$,

$$c = u\frac{\Delta t}{\Delta x} \text{ and } s = \alpha\frac{\Delta t}{(\Delta x)^2}, \tag{49}$$

where $\bar\phi$ denotes the approximate value of ϕ.

4.1 Consistency analysis

A formal consistency analysis of (48) shows that it is consistent with the ADE, with a truncation error given by

$$E(x,t) = \frac{1}{2}\psi u\Delta x\frac{\partial^2\phi}{\partial x^2} - \frac{1}{2}\Delta t\frac{\partial^2\phi}{\partial t^2} + O\{(\Delta x)^2, (\Delta t)^2\}. \tag{50}$$

A rearrangement of the ADE, differentiating the terms in the equation, and substituting into (50) yields

$$E(x,t) = \frac{1}{2}u(\psi\Delta x - u\Delta t)\frac{\partial^2\phi}{\partial x^2} + O\{\Delta t, (\Delta x)^2\}. \quad (51)$$

Thus, $E(x,t) \to 0$ as $\Delta x \to 0$ and $\Delta t \to 0$, confirming that equation (48) is consistent with the ADE. However, since Δx and Δt are finite we are actually solving the equation with additional terms on the right side, namely

$$\frac{\partial\phi}{\partial t} + u\frac{\partial\phi}{\partial x} = (\alpha + \alpha')\frac{\partial^2\phi}{\partial x^2} + O\{\Delta t, (\Delta x)^2\} \quad (52)$$

where

$$\alpha' = \frac{1}{2}u(\psi\Delta x - u\Delta t), \quad (53)$$

referred to as artificial diffusion, is the change in the diffusion coefficient α introduced by the use of (48). We note that setting $\psi = 1$ yields the so-called *upwind scheme*, which is diffusive, whereas $\psi = 0$ produces the FTCS (forward in time, centered in space) scheme, which can lead to negative diffusion. An optimal scheme that eliminates artificial diffusion is obtained by setting

$$\psi\Delta x - u\Delta t = 0 \quad \Longrightarrow \psi = u\frac{\Delta t}{\Delta x} = c, \quad (54)$$

to get:

$$\bar{\phi}_j^{n+1} = \left[s + \frac{1}{2}(1+c)c\right]\bar{\phi}_{j-1}^n + (1 - 2s - c^2)\bar{\phi}_j^n + \left[s - \frac{1}{2}(1-c)c\right]\bar{\phi}_{j+1}^n. \quad (55)$$

4.2 Stability analysis

A von Neumann stability analysis gives the stability region of (55) to be

$$0 < 2s \leq 1 - c^2, \quad (56)$$

as depicted in Figure 1. Details of the stability analysis that produced (56) can be found in [1] (their Appendix B). A discretized equation of the Peclet-form of the ADE is provided in Appendix A.3, and compared to the discretized native-form of the equation.

The optimal explicit scheme is second-order accurate in space as depicted in Figure 2, where we plot the absolute error, $|E|$, between the numerical and the analytic solution (equation (39)) at the center of the domain ($x = 0.5$) at a final time of $t = 1.0$ against the grid spacing. Keeping a fixed value of the diffusion parameter $s = 1/4$, and varying the advection parameter, c, we find that the equation of best fit for each c yields a power for Δx in the range $1.98 - 3.02$ (Figure 2a). For example, at $s = 1/4$ and $c = 0.01$, the relationship between the error and grid spacing is

$$E = 9.03(\Delta x)^{2.03}.$$

At a fixed value of $c = 1/4$, the equation of best fit for each s yields $O(\Delta x)^{3.02}$, indicating a much lower discretization error (Figure 2b).

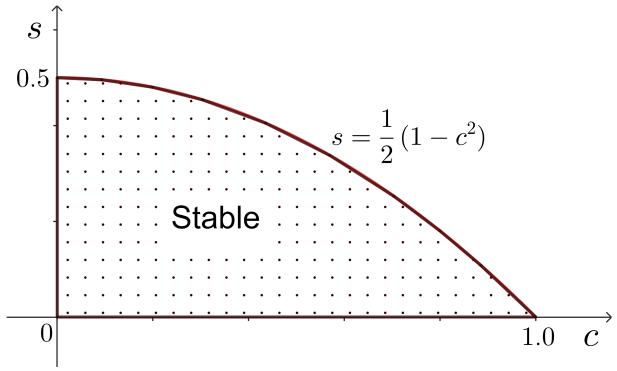

Fig. 1: Stability region for the optimal explicit method of solving the ADE.

5 Discussion of results

The evolution of $\phi(x,t)$ from three analytic solutions and the optimal numerical scheme is displayed in Figure 3. The numerical solution closely matches the analytic solution of [5] (see equation (42)) throughout the period of evolution. The solution obtained by [7] deviates from the other analytic solutions for $t < 0.5$, due to the discontinuity at the end points. Thus, analytic solutions that lack continuity of $\phi(x,t)$ at the end points are challenging to use in comparing to numerical methods for purposes of evaluation. Kim's solution matches up closely to the other analytic solutions for $t \geq 0.5$. This implies that care must be taken in comparing analytic solutions to numerical solutions or observational data if the solutions are discontinuous at the end points.

The time evolution of $\phi(x,t)$ for nonzero exit boundary and initial values of $\phi_1 = 0.3 = w_0$, and a decaying inlet boundary value with $\gamma = 2$ are shown in Figure 4. As expected, both the analytic and numerical solutions show a decrease in the level of $\phi(x,t)$ with time throughout the domain, except at the nonzero exit boundary which maintains its prescribed value.

A contour map showing the time evolution of $\phi(x,t)$ for all times in the range $0 \leq t \leq 1$ is displayed in Figure 5. Apart from the fixed value at the exit boundary, the largest values of $\phi(x,t)$ occur for times less than about $t = 0.5$, after which the values decrease towards zero at almost everywhere except in the region closer to the exit boundary..

The analytic and numerical values of $\phi(x,t)$ may become negative at some times and spatial positions depending on the parameters utilized. For example, at $t = 0.0001$, $x = 0.9899$ and $Pe = 70$, equation (42) gives a value of $\phi(x,t) = -0.24$. However, in this case, the negative values disappear at longer times ($t \geq 0.002$; not shown here). Since in many practical applications, such as the transport of pollutants, negative values of $\phi(x,t)$ have no physical meaning, care must be taken in applying the analytic and numerical solutions of the ADE. Such

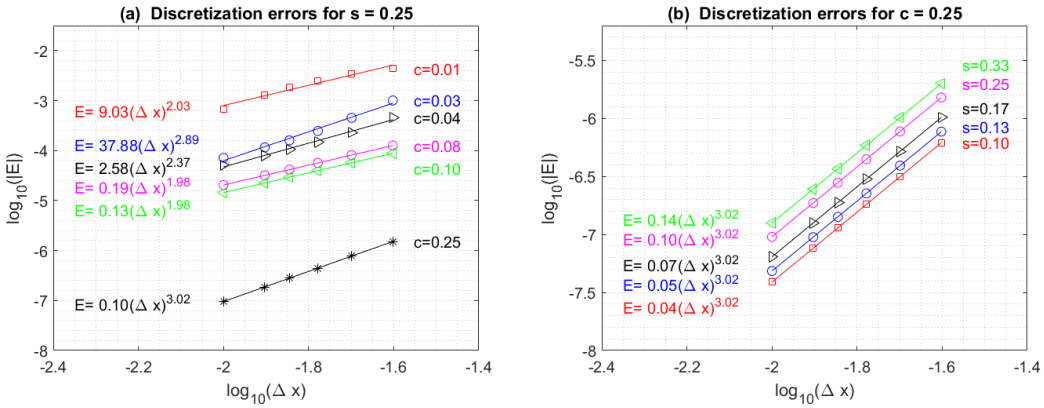

Fig. 2: The discretization error $|E|$ plotted against grid spacing Δx using the optimal technique of solving the ADE for (a) fixed $s = 1/4$ and varying c, and (b) for fixed $c = 1/4$ and varying s. The linear relationship of best fit between E and Δx are displayed on each plot, indicating second-order accuracy on average. Here $\gamma = 0.5$ and $w_0 = 0.2$.

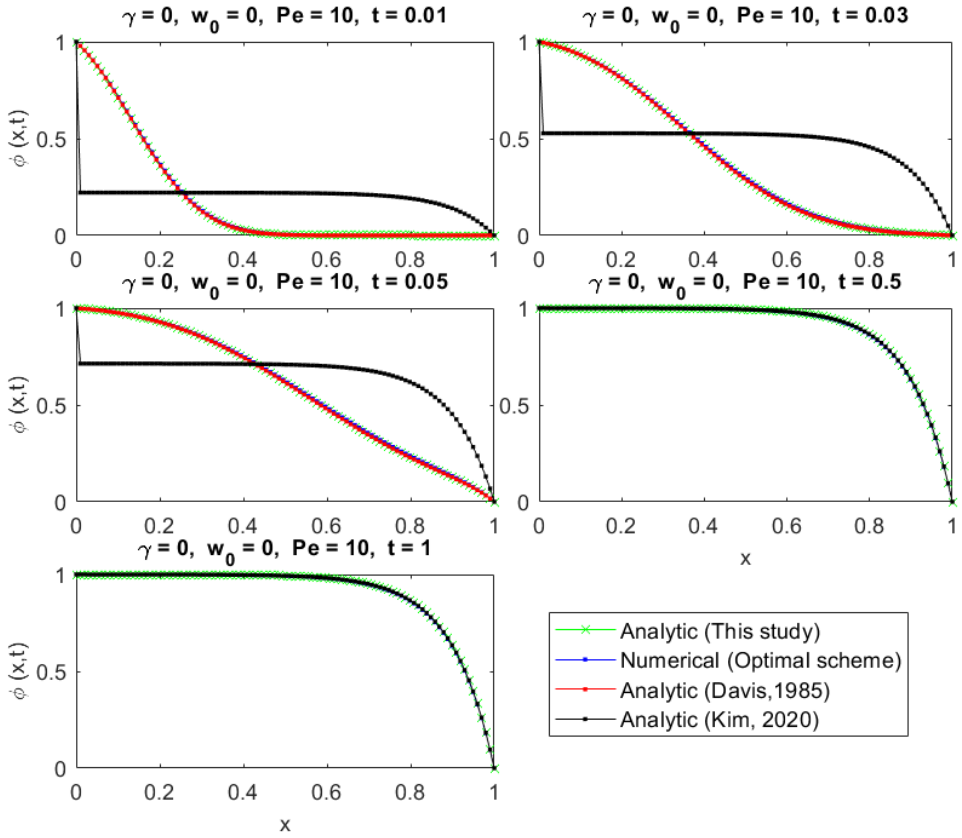

Fig. 3: Analytic and numerical solutions to the ADE at various times for $\gamma = 0$, $\phi_0 = 1$, $\phi_1 = w_0 = 0$, $\Delta x = 0.01$, and $\Delta t = 2.5 \times 10^{-5}$.

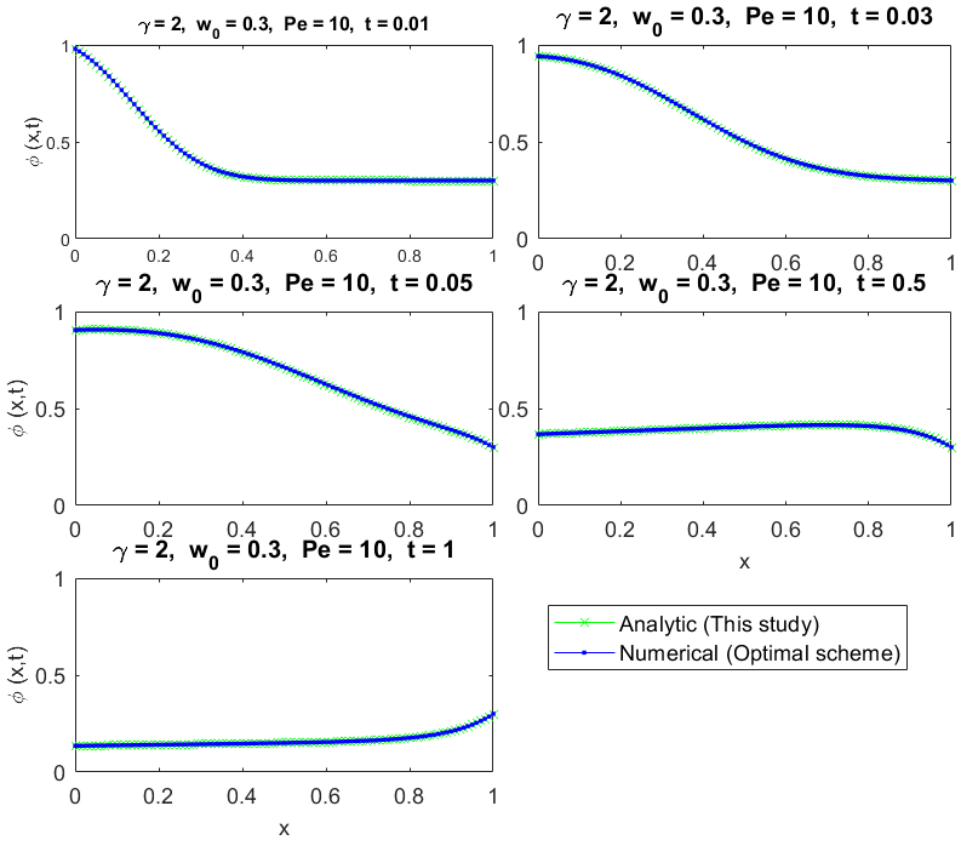

Fig. 4: Analytic and numerical solutions to the ADE at varying times for $\gamma = 2$, $\phi_0 = 1$, $\phi_1 = w_0 = 0.3$, $\Delta x = 0.01$, and $\Delta t = 2.5 \times 10^{-5}$.

negative values have also been reported in other studies (e.g., [10]).

6 Conclusions

The Laplace transform method is used to derive an analytical solution to the one-dimensional advection–diffusion equation (ADE) in a bounded domain with an exponentially decaying inlet boundary condition, yielding a solution that is continuous at both endpoints, unlike previous approaches [7, 12], which result in discontinuities at the boundaries. The solution derived in this paper is used to explain the source of the discrepancy between the continuous and discontinuous solutions. The continuous solution is consistent with that of [5] for fixed inlet boundary conditions. Analytic solutions are generally useful for comparison to numerical solutions to determine the accuracy of a numerical method. Thus, we also employed an explicit finite difference numerical technique [9] to solve the problem and compared that to the analytic solutions. The numerical solution is second-order accurate and matches the analytic solution quite well. Even though analytic solutions with discontinuities at one or both end points are useful and have been derived and utilized (e.g., [3] (section 4.7, page 144), [8], [7], [12]), it is important under many circumstances to obtain analytic solutions that are continuous at the end points.

Two forms of non-dimensional advection-diffusion equations are often presented in the literature; the native form where the resulting equation has a similar form as the dimensional equation, and the Peclet form which results in a single coefficient in terms of the Peclet number. We have established the relationship between these two forms to make it easier for purposes of analytical and numerical comparisons. We recognized that there are other ways to non-dimensionalize the ADE besides those presented here, and we hope our approach would provide some guidance when confronted with other forms of the non-dimensional equation.

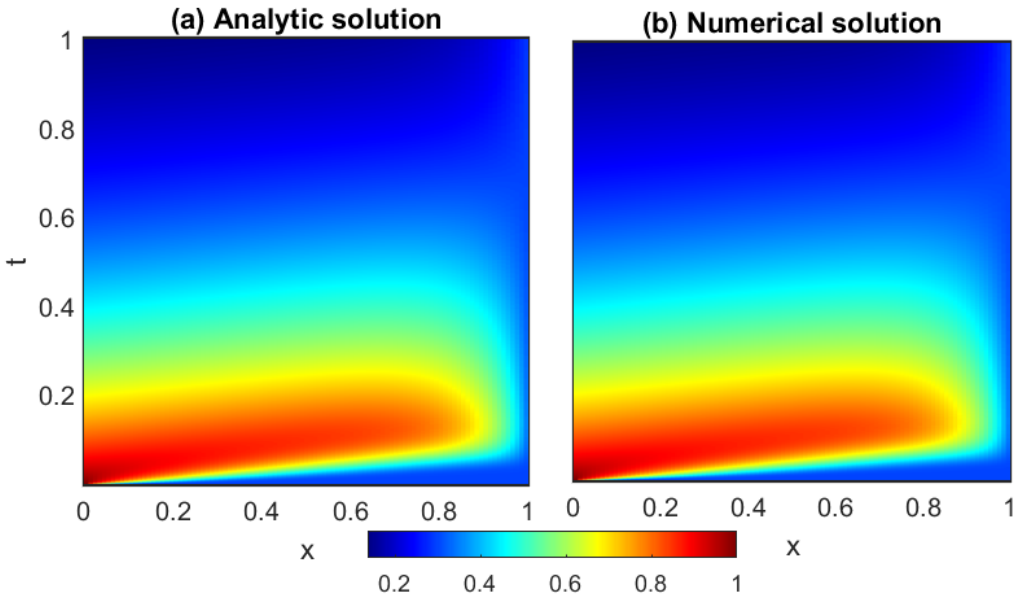

Fig. 5: Same as in Figure 4, but for all times in the range $0 \leq t \leq 1$.

Acknowledgement

The authors sincerely thank the anonymous referee for a careful reading of the manuscript and for constructive comments that significantly improved the paper.

References

[1] J. K. Ansong, F. Obeng-Forson, and V. T. Teyekpiti. A note on the solution to a 1D advection–diffusion equation with exponentially decaying inlet boundary condition. *Scientific African*, 30, 2025.

[2] H. Brenner. The diffusion model of longitudinal mixing in beds of finite length numerical values. *Chem. Engng. Sci.*, 17, 1962.

[3] H. S. Carslaw and J. C. Jaeger. *Conduction of Heat in Solids*. Oxford University Press, p. 144, equation (4), 1986.

[4] R. W. Cleary and D. D. Adrian. Analytical Solution of the Convective-Dispersive Equation for Cation Adsorption in Soils. *Soil Science Society of America Proceedings*, 37, 1973.

[5] G. B. Davis. A laplace transform technique for the analytical solution of a diffusion-convection equation over a finite domain. *Applied mathematical modelling*, 9(1):69–71, 1985.

[6] A. Erdelyi, W. Magnus, F. Oberhettinger, and F. Tricomi. *Tables of integral transforms, Vol. I*. McGraw-Hill, New York, p. 259, No (39), 1954.

[7] A. S. Kim. Complete analytic solutions for convection-diffusion-reaction-source equations without using an inverse Laplace transform. *Scientific Reports*, 10(1):1–13, 2020.

[8] Mohammad Farrukh N Mohsen and Mohammed H Baluch. An analytical solution of the diffusion-convection equation over a finite domain. *Applied Mathematical Modelling*, 7(4):285–287, 1983.

[9] J. Noye. Finite difference methods for solving the one-dimensional transport equation. In *North-Holland Mathematics Studies*, volume 145, pages 231–256. Elsevier, 1987.

[10] J. Noye. A new third-order finite-difference method for transient one-dimensional advection-diffusion. *Communications in Applied Numerical Methods*, 6, 1990.

[11] Obeng-Forson. *Analytical solutions to a 1D advection-diffusion equation and comparison to observations*. University of Ghana, MPhil Thesis, 2022.

[12] F. Obeng-Forson and J. K. Ansong. Mathematical modeling of pollutant transport in river Fena in Ghana. *Science and Development Journal*, 6(1):13–26, 2022.

[13] M. Th. van Genuchten and W. J. Alves. *Analytical solutions of the one-dimensional convective-dispersive solute transport equation*. Number 1661. US Department of Agriculture, Agricultural Research Service, 1982.

A Appendix

A.1 Fourier series expansion of sine hyperbolic functions

We seek the Fourier series sine expansions of

$$g(x)=\frac{\sinh[\lambda(1-x)]}{\sinh(\lambda)} \text{ and } h(x)=\frac{\sinh(\lambda x)}{\sinh(\lambda)}, \tag{57}$$

where $0\le x\le 1$. Now, by definition, the Fourier series expansion of

$$f(x)=\sinh[\lambda(1-x)], \qquad 0\le x\le 1. \tag{58}$$

is given by

$$f(x)=\sum_{n=1}^{\infty} b_n \sin(n\pi x) \tag{59}$$

where

$$b_n=2\int_0^1 \sinh[\lambda(1-x)]\sin(n\pi x)\,dx. \tag{60}$$

Let $u=1-x \quad \Longrightarrow du=-dx$, and thus

$$\begin{aligned} b_n &= -2\int_1^0 \sinh(\lambda u)\sin[n\pi(1-u)]\,du \\ &= 2\int_0^1 \sinh(\lambda u)\sin[n\pi(1-u)]\,du. \end{aligned}$$

Expanding $\sin[n\pi(1-u)]$ and substituting into the integral gives

$$b_n=-2\cos(n\pi)\int_0^1 \sinh(\lambda u)\sin(n\pi u)\,du. \tag{61}$$

Using the following identity from tables of integrals:

$$\int \sinh(ax)\sin(cx)\,dx=\frac{a\cosh(ax)\sin(cx)}{a^2+c^2}-\frac{c\sinh(ax)\cos(cx)}{a^2+c^2}, \tag{62}$$

and setting $a=\lambda$ and $c=n\pi$ in (62), yields

$$\begin{aligned} &\int_0^1 \sinh(\lambda x)\sin(n\pi x)\,dx= \\ &\left[\frac{\lambda\cosh(\lambda x)\sin(n\pi x)}{\lambda^2+(n\pi)^2}-\frac{n\pi\sinh(\lambda x)\cos(n\pi x)}{\lambda^2+(n\pi)^2}\right]_0^1 \\ &=\frac{-n\pi\sinh(\lambda)\cos(n\pi)}{\lambda^2+(n\pi)^2}. \end{aligned} \tag{63}$$

Substituting (63) into (61) gives

$$\begin{aligned} b_n &= 2\cos(n\pi)\frac{n\pi\sinh(\lambda)\cos(n\pi)}{\lambda^2+(n\pi)^2} \\ &= 2\pi\frac{n\sinh(\lambda)}{\lambda^2+(n\pi)^2} \end{aligned} \tag{64}$$

since $\cos(n\pi)=(-1)^n \Longrightarrow \cos(n\pi)^2=1$. Substitute equation (64) into (59) to get

$$f(x)=\sinh[\lambda(1-x)]=2\pi\sum_{n=1}^{\infty}\frac{n\sinh(\lambda)}{\lambda^2+(n\pi)^2}\sin(n\pi x). \tag{65}$$

Hence,

$$\frac{\sinh[\lambda(1-x)]}{\sinh(\lambda)}=2\pi\sum_{n=1}^{\infty}\frac{n\sin(n\pi x)}{\lambda^2+(n\pi)^2}. \tag{66}$$

Similarly, we have

$$\frac{\sinh(\lambda x)}{\sinh(\lambda)}=2\pi\sum_{n=1}^{\infty}\frac{n\sin[n\pi(1-x)]}{\lambda^2+(n\pi)^2}. \tag{67}$$

A.2 Some Inverse Laplace Transforms from Tables

From [6] (Vol. I, page 259, equation (39)), we have

$$\begin{aligned} &\mathscr{L}^{-1}\left\{\frac{1}{p-i\omega}\frac{\sinh(xp^{1/2})}{\sinh(lp^{1/2})}\right\}=\frac{\sinh(xi^{1/2}\omega^{1/2})}{\sinh(li^{1/2}\omega^{1/2})}e^{i\omega t} \\ &+2\pi\sum_{n=1}^{\infty}\frac{n(-1)^n\sin(n\pi x/l)}{n^2\pi^2+i\omega l^2}e^{-n^2\pi^2 t/l^2}, \end{aligned} \tag{68}$$

where $l\ge x>0$ and p is the Laplace transform variable of t. Now, if we let $l=1$ and $\omega=-ib$, we get

$$\begin{aligned} &\mathscr{L}^{-1}\left\{\frac{1}{p-b}\frac{\sinh(p^{1/2}x)}{\sinh(p^{1/2})}\right\}=\frac{\sinh(b^{1/2}x)}{\sinh(b^{1/2})}e^{bt} \\ &+2\pi\sum_{n=1}^{\infty}\frac{n(-1)^n\sin(n\pi x)}{b+n^2\pi^2}e^{-n^2\pi^2 t}, \end{aligned} \tag{69}$$

where $0<x\le 1$. By replacing x by $1-x$, we get

$$\begin{aligned} &\mathscr{L}^{-1}\left\{\frac{1}{p-b}\frac{\sinh[p^{1/2}(1-x)]}{\sinh(p^{1/2})}\right\}=\frac{\sinh[b^{1/2}(1-x)]}{\sinh(b^{1/2})}e^{bt} \\ &+2\pi\sum_{n=1}^{\infty}\frac{n(-1)^n\sin[n\pi(1-x)]}{b+n^2\pi^2}e^{-n^2\pi^2 t}. \end{aligned} \tag{70}$$

$$\begin{aligned} &\mathscr{L}^{-1}\left\{\frac{1}{p-b}\frac{\sinh[p^{1/2}(1-x)]}{\sinh(p^{1/2})}\right\}=\frac{\sinh[b^{1/2}(1-x)]}{\sinh(b^{1/2})}e^{bt} \\ &-2\pi\sum_{n=1}^{\infty}\frac{n\sin(n\pi x)}{b+n^2\pi^2}e^{-n^2\pi^2 t}, \end{aligned} \tag{71}$$

where $0<x\le 1$, and we used

$$\sin[n\pi(1-x)]=-\cos(n\pi)\sin(n\pi x)=(-1)^{n+1}\sin(n\pi x).$$

A.3 Discretization of the Peclet form

Consider the nondimensional 1D ADE given in what we refer to as the Peclet-form:

$$\frac{\partial \phi}{\partial t} + P_e \frac{\partial \phi}{\partial x} = \frac{\partial^2 \phi}{\partial x^2} \tag{72}$$

for $0 < x < 1$ and P_e is the Peclet number. Here, the forward difference is used for the time derivative, the centered difference is applied to the second-order spatial derivative, and a weighted combination of backward and centered differences is employed for the first-order spatial derivative, namely

$$\frac{\partial \phi}{\partial x}\Big|_j^n = \psi \frac{\partial \phi}{\partial x}\Big|_j^n + (1-\psi)\frac{\partial \phi}{\partial x}\Big|_j^n, \quad 0 \le x \le 1. \tag{73}$$

The backward difference is used for the spatial derivative term with coefficient ψ, while the centered difference is applied to the term associated with the weight $(1-\psi)$, yielding

$$\begin{aligned} &\frac{\phi_j^{n+1} - \phi_j^n}{\Delta t} + O\{\Delta t\} + P_e \left[\psi \left(\frac{\phi_j^n - \phi_{j-1}^n}{\Delta x} + O\{\Delta x\} \right) \right. \\ &\left. + (1-\psi) \left(\frac{\phi_{j+1}^n - \phi_{j-1}^n}{2\Delta x} + O\{(\Delta x)^2\} \right) \right] \\ &= \left[\frac{\phi_{j+1}^n - 2\phi_j^n + \phi_{j-1}^n}{(\Delta x)^2} + O\{(\Delta x)^2\} \right] \end{aligned} \tag{74}$$

Neglecting the terms of order $O\{\Delta t, \psi \Delta x, (1-\psi)(\Delta x)^2\}$ and rearranging, produces the explicit finite difference equation

$$\begin{aligned} \bar{\phi}_j^{n+1} &= \left[\hat{s} + \frac{1}{2}(1+\psi)\hat{c} \right] \bar{\phi}_{j-1}^n + (1 - 2\hat{s} - \psi\hat{c})\bar{\phi}_j^n + \\ &\left[\hat{s} - \frac{1}{2}(1-\psi)\hat{c} \right] \bar{\phi}_{j+1}^n \end{aligned} \tag{75}$$

where $j = 1, 2, \cdots, J-1$,

$$\hat{c} = P_e \frac{\Delta t}{\Delta x} \text{ and } \hat{s} = \frac{\Delta t}{(\Delta x)^2}, \tag{76}$$

where $\bar{\phi}$ denotes the approximate value of ϕ. Note that the form of (75) is the same as for (48), the difference being the definitions in (76) as compared to (49).

If P_e is replaced by $P_e = 2\lambda$ in (72), the weighted-average scheme becomes

$$\begin{aligned} \bar{\phi}_j^{n+1} &= [\bar{s} + (1+\psi)\bar{c}]\,\bar{\phi}_{j-1}^n + (1 - 2\bar{s} - 2\psi\bar{c})\bar{\phi}_j^n \\ &+ [\bar{s} - (1-\psi)\bar{c}]\,\bar{\phi}_{j+1}^n \end{aligned} \tag{77}$$

where

$$\bar{c} = \lambda \frac{\Delta t}{\Delta x} \text{ and } \bar{s} = \frac{\Delta t}{(\Delta x)^2}. \tag{78}$$

Comparing the two schemes, (48) and (77), shows that

$$\bar{c} = \frac{1}{2}c \implies c = 2\bar{c}. \tag{79}$$

Thus, for an optimal scheme, we set

$$\psi = c = 2\bar{c} \tag{80}$$

in (77) to get

$$\begin{aligned} \bar{\phi}_j^{n+1} &= [\bar{s} + (1+2\bar{c})\,\bar{c}]\,\bar{\phi}_{j-1}^n + [1 - 2\bar{s} - (2\bar{c})^2]\bar{\phi}_j^n \\ &+ [\bar{s} - (1-2\bar{c})\bar{c}]\,\bar{\phi}_{j+1}^n \end{aligned} \tag{81}$$

Joseph K. Ansong is a Senior Lecturer and Head of the Department of Mathematics at the University of Ghana, Legon. He earned his PhD in Applied Mathematics from the University of Alberta, Canada, and his MSc in Engineering Mathematics from the University of Twente, the Netherlands. His research focuses on understanding how physical processes influence the spread, dilution, and persistence of contaminants in the atmosphere and water bodies. He also works on the development and analysis of mathematical models for flood dynamics, and applies numerical modeling techniques to the study of geophysical flows, including coastal upwelling.

Ferdinard Obeng-Forson holds an MPhil in Mathematics from the University of Ghana. He has a strong background in academic research and applied analytical work, with particular interest in mathematical modeling and the use of analytical and numerical methods for partial differential equations. His research focus also extends to fluid dynamics and its applications to real-world systems. He is an early-career researcher with four publications in reputable applied mathematics journals and is actively engaged in research, technical reporting, and professional development, with a strong interest in applying mathematical tools to interdisciplinary and applied problems.